Quantum wave turbulence

M. B. Haeri* and S. J. Putterman
Department of Physics, University of California, Los Angeles, California 90024

A. Garcia
Department of Physics, San Jose State University, California 95192

P. H. Roberts
Department of Mathematics, University of California, Los Angeles, California 90024
(Received 28 July 1992)

The nonlinear quantum kinetic equation for the interaction of sound waves is solved via analytic and numerical techniques. In the classical regime energy cascades to higher frequency (ω) according to the steady-state power law $\omega^{-3/2}$. In the quantum limit, the system prefers a reverse cascade of energy which follows the power law ω^{-6}. Above a critical flux, a new type of spectrum appears which is neither self-similar nor close to equilibrium. This state of nonlinear quantum wave turbulence represents a flow of energy directly from the classical source to the quantum degrees of freedom.

PACS number(s): 47.25.−c, 03.40.Kf, 03.65.−w

The anharmonic terms in the Hamiltonian for fluid mechanics account for the scattering of one sound wave by another. In the classical limit this nonlinear effect is referred to as the wave-wave interaction [1], and in the quantum limit is referred to as the phonon-phonon interaction [2]. For fluids [3] and more complex systems [4] the quantum and classical regimes can be bridged by a single kinetic equation, which describes the nonlinear time development of the spectral intensity with effects due to scattering of acoustic energy by the zero-point motion [5].

We used this kinetic equation to study the fate of acoustic energy injected into a fluid so as to drive it far off equilibrium. In the classical region of wave-number space, energy cascades from low to high frequency to generate a steady-state power-law distribution (see Fig. 1) [6] analogous to the Kolmogorov spectrum [7] of vortex turbulence. Classical wave turbulence accounts for the spectrum of wind-driven surface waves in the ocean [8] and Alfvén waves driven by the solar wind [9]. In the quantum region there is a reverse cascade of energy from high to low frequency. The steady state of quantum wave turbulence is also characterized by a power-law dependence for the spectral intensity (see Fig. 2). We believe

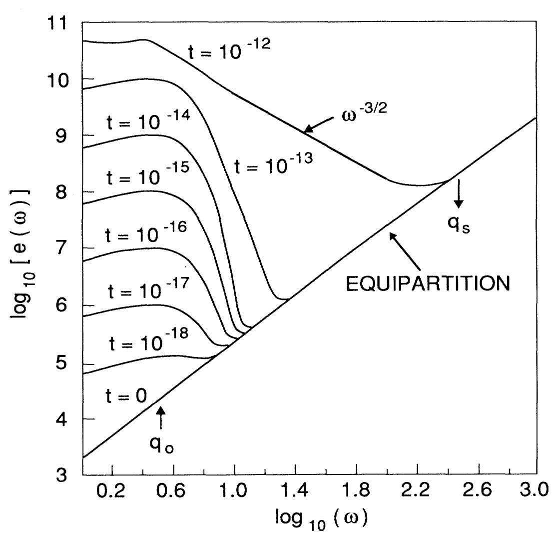

FIG. 1. Time evolution of the classical wave turbulent spectrum from an initial Rayleigh-Jeans distribution with $T=2000$ to a steady-state spectral density that follows a $-\frac{3}{2}$ power law. An energy flux of 10^{24} is injected over a Gaussian distribution of modes centered around $\omega=3$ and removed over a distribution of modes greater than 300.

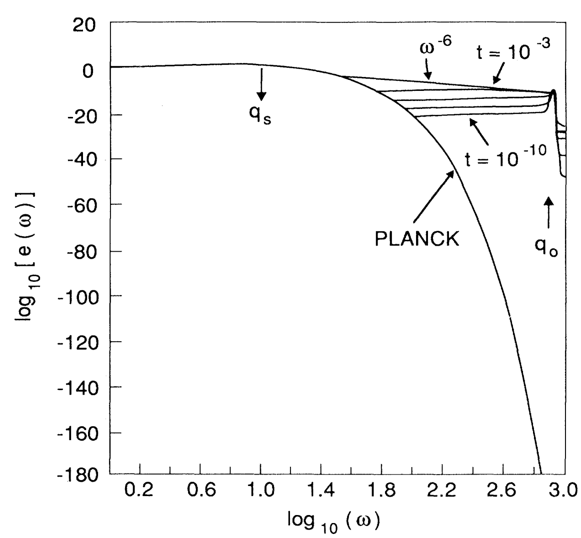

FIG. 2. Time evolution of the quantum wave turbulent spectrum from an initial Planck distribution with $T=1.5$ to a steady-state spectral density that follows a -6 power law. An energy flux of 1000 is injected over a Gaussian distribution of modes centered around $\omega=800$ and removed over a Gaussian distribution of modes centered at $\omega=10$.

that this reverse quantum cascade underlies the measured high-frequency phonon-redistribution processes [10,11]. When the input of low-frequency energy exceeds a critical value, it is possible to realize a cascade where energy is mechanically transported directly from the classical to the quantum domain (see Fig. 3).

To study quantum wave turbulence we consider the mutual interactions of a "sea" of dispersionless waves. The lack of dispersion for acoustic waves implies that wave action I changes as a result of nonlinear three-wave resonant interactions described by the kinetic equation [2,3,5]

$$\frac{\partial I(\omega_n)}{\partial t}=\frac{2\pi^3G^2c}{\rho V^2}\left\{\int_0^{\omega_n}\{I(\omega_n-\omega_k)I(\omega_k)-I(\omega_n)[I(\omega_k)+I(\omega_n-\omega_k)+\hbar]\}\sigma(\omega_n-\omega_k)\sigma(\omega_k)d\omega_k \right.$$
$$\left. +2\int_0^{\infty}\{I(\omega_n+\omega_k)[I(\omega_k)+I(\omega_n)+\hbar]-I(\omega_k)I(\omega_n)\}\sigma(\omega_n+\omega_k)\sigma(\omega_k)d\omega_k\right\}, \tag{1}$$

where $\sigma(\omega)=V\omega^2/2\pi^2c^3$ is the density of states, V is the container volume, ρ is the density, $G=1+(\rho/c)dc/d\rho$ is the Gruneisen coefficient which determines the coupling between modes, $\hbar$ is Planck's constant, c is the speed of sound, and ω_k is the frequency of the mode with wave number k. In parallel with Boltzmann's equation, a discretization of Eq. (1) requires that higher-order correlations be neglected [1,12] (Stosszahl ansatz). The energy per unit volume per unit frequency interval (i.e., spectral intensity) is $e(\omega)=I(\omega)\omega\sigma(\omega)/V$.

The equilibrium solution to (1) is the Planck spectrum $I(\omega)=\hbar/[\exp\{\hbar\omega/k_BT\}-1]$, where k_B is Boltzmann's constant and T is the temperature. For small $\hbar$, $e(\omega)\to k_BT\omega^2/2\pi^2c^3$, which is equipartition of energy. For $\hbar\omega/k_BT\gg 1$, $I\to\hbar\exp(-\hbar\omega/k_BT)$, which is Wien's law.

The analytic solutions for wave turbulence follow from the conservation of wave energy with respect to its flow in phase space [6],

$$\frac{\partial e(\omega_n)}{\partial t}+\frac{\partial q(\omega_n)}{\partial\omega_n}=0\ , \tag{2}$$

where $q(\omega)$ is the energy throughput (erg/cm^3 sec). In the steady state $q=q_0$ is a constant; thus (2) yields

$$q_0=-\frac{1}{2\pi^2c^3}\int\omega_n^3\frac{\partial I(\omega_n)}{\partial t}d\omega_n\ , \tag{3}$$

where $\partial I(\omega_n)/\partial t$ refers to the right-hand side of (1). The classical limit of (3) involves the quadratic terms in I which balance when I is proportional to $\omega^{-9/2}$. The strong quantum limit of (3) involves the linear terms in (1) which balance for I proportional to ω^{-9}. Substituting these forms for the solution into (3) recovers the known steady-state spectrum for classical wave turbulence [6],

$$e(\omega)=\frac{A(\rho c^2q_0)^{1/2}}{\sqrt{\pi}|G|\omega^{3/2}}\ , \tag{4}$$

as well as the quantum power spectrum of off-equilibrium noise,

$$e(\omega)=\frac{a_0 2\pi q_0c^5\rho}{\hbar G^2\omega^6}\ . \tag{5}$$

In (4) the constant $A\approx 1/(52.42)^{1/2}\approx 0.138^{12}$ and in (5) the constant $a_0=1800/37$. These solutions apply when $e(\omega)$ is large compared with its equilibrium value.

We now turn to the numerical solution of Eq. (1). These solutions (i) verify the validity of the steady-state cascades (4) and (5), (ii) elucidate the temporal development of the classical and quantum off-equilibrium spectra, and (iii) determine the spectrum of wave turbulence at the interface of classical and quantum mechanics. Numerical solutions of the strictly classical kinetic equation verified the exponent in the steady-state spectrum [14,15].

The nonlinear coupling of the classical and quantum domains [case iii] are appreciated by comparing Eq. (4) and the Planck spectrum. If the low-frequency input flux (q_0) is larger than a critical flux q_c, the distribution (4) goes over the top of the spectrum where the equilibrium energy is a maximum (and $\omega=\omega_p=2.88k_BT/\hbar$). The critical flux q at which (4) is tangent to the Planck spectrum is

$$q_c=A_0\frac{G^2(k_BT)^9}{\rho c^8\hbar^7}\ , \tag{6}$$

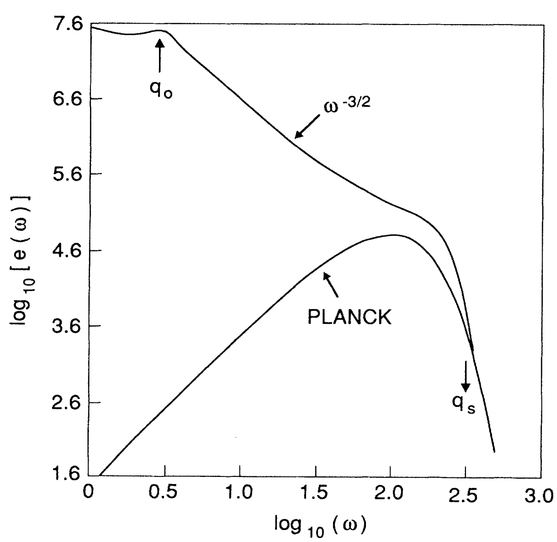

FIG. 3. Forward cascade of energy from the classical regime to the quantum regime for $q>q_c$. An energy flux equals 10^{17} is input over a Gaussian distribution of modes centered at $\omega=3$ and removed over modes greater than $\omega=300$. The spectrum follows a $-\frac{3}{2}$ power law which then turns down with a slope steeper than Wien's law so as to meet the initial Planck distribution with $T=35$.

where A_0 is a constant. For this parameter range the motion is quantum and nonlinear. Except for a different proportionality constant, these considerations also apply to the reverse flux spectrum.

The continuous kinetic equation was discretized by solving for the action at N uniformly spaced frequencies, with grid spacing Δ, and by using a trapezoidal rule to evaluate the integrals in (1). A merit of this method is that the equilibrium solution of (7) is the Planck spectrum. A source for injecting energy and a sink for removing energy were added to (1) to yield

$$\frac{\partial I_i}{\partial t} = \sum_{j=1}^{i=1} j^2(i-j)^2\{I_j I_{i-j} - I_i(I_{i-j}+I_j+1)\} + 2\sum_{j=1}^{N-i} j^2(i+j)^2\{I_{i+j}(I_i+I_j+1) - I_i I_j\} + q_0 k_0^{-3}\delta_{i,k_0} - q_s k_s^{-3}\delta_{i,k_s} . \quad (7)$$

In deriving (7) we introduced the dimensionless time ($\bar{t}$), temperature $\bar{T}$, flux ($\bar{q}$), action ($\bar{I}$), and spectral density ($\bar{e}$):

$$\bar{t} = \frac{tG^2\Delta^5\mathcal{J}}{2\pi c^5\rho}, \quad \bar{T} = \frac{k_B T}{\hbar\Delta}, \quad \bar{q} = \frac{q4\pi^3c^8\rho}{G^2\Delta^9\mathcal{J}^2}, \quad \bar{I} = \frac{I}{\mathcal{J}}, \quad \bar{e}_j = j^3\bar{I}_j \quad (8)$$

where the characteristic action $\mathcal{J}$ is $k_B T/N\Delta$ in the classical limit ($\bar{T}/N > 1$) and $\mathcal{J} = \hbar$ in the quantum limit $\bar{T}/N \ll 1$ [in (7) we have displayed the case $\mathcal{J} = \hbar$]. The mode numbers for the source and sink are k_0 and k_s, and $\bar{\omega} = \omega/\Delta$. In discretizing (1), ω_j is replaced by Δj and $Ij = I(j\Delta)$. In (7) and in what follows and in the figures the bars were dropped.

Expression (7) was implemented on an Alliant *FX*-80 computer and solved for $N = 1000$. The Planck distribution is the initial condition. The initial bath temperature T was controlled to access the classical, strong quantum, and nonlinear quantum regimes. Here, the classical region is where in equilibrium all 1000 modes follow a Rayleigh-Jeans type of distribution; in the strong quantum regime most of the 1000 modes follow Wien's law in equilibrium; in the nonlinear quantum regime a Planck distribution must be used.

Figure 1 depicts the time evolution of the classical spectrum from an initial Rayleigh-Jeans distribution with $T = 2000$ to a steady-state ($t = 10^{-12}$) spectral energy distribution following a $-\frac{3}{2}$ power law in the nonlinear cascade regime between $\omega = 10$ and 100. A flux of 10^{24} was supplied over a Gaussian distribution of modes centered at $\omega = 3$ and subsequently removed over modes greater than 300 so as to preserve the initial temperature of the Rayleigh-Jeans distribution at high frequencies. The $-\frac{3}{2}$ power law is achieved to three digits accuracy, and the Kolmogorov constant for acoustic turbulence $A \approx 0.15$. This value approaches the analytic value of A given in (4) as T increases. Steady states characterized by a reverse flux of energy can also be achieved in the classical regime, but these fluxes are down by at least a factor of 10^7.

As an example of recovering the physical variables take $\rho = 1.0$ g/cm^3, $c = 10^4$ cm/sec, and $\Delta = 10^6$ Hz so that $T = 20$ mK. Then a dimensionless time of order 10^{-13} corresponds to a real time of 10^4 s and flux of order 10^{24} corresponds to a Mach number of order 10^{-6}. For a real system N can be much larger, but we claim that the qualitative insights obtained with $N = 1000$ will remain valid.

The time evolution of the quantum spectrum from an initial Planck distribution with $T = 1.5$ to a steady-state ($t = 10^{-3}$) spectral energy distribution following a steep -6 power of the frequency between $\omega = 700$ and 40 (inertial range) is shown in Fig. 2. Unlike the classical case, a reverse cascade of energy is preferred. This is consistent with observations of spontaneous decay of high-frequency phonons [10,11,13]. The numerically computed constant is the same as a_0 in expression (5) to three digits.

In the nonlinear quantum regime ($q \geq q_c$) neither the linear nor quadratic terms can be neglected; the spectrum is neither self-similar nor close to equilibrium. Thus our only means of investigating the response in this region is numerical.

Consider the case where energy is injected at small ω and removed at ω_p. As q increases, the value $q = q_c \approx 60T^9$ is eventually reached. At this value the off-equilibrium spectrum follows the $-\frac{3}{2}$ power law at low ω and then turns up to become tangent to the Planck spectral peak as shown in Fig. 4, plot A (for this plot $q = 6\times10^{19} \approx q_c$ and $T = 100$). Note, that even if energy were removed at frequencies higher than ω_p, the steady-state spectrum would have the same form provided $q \leq q_c$. Also shown in Fig. 4 (plot B) is the case where $q = 5\times10^{20} > q_c$; the spectrum follows a $-\frac{3}{2}$ power law

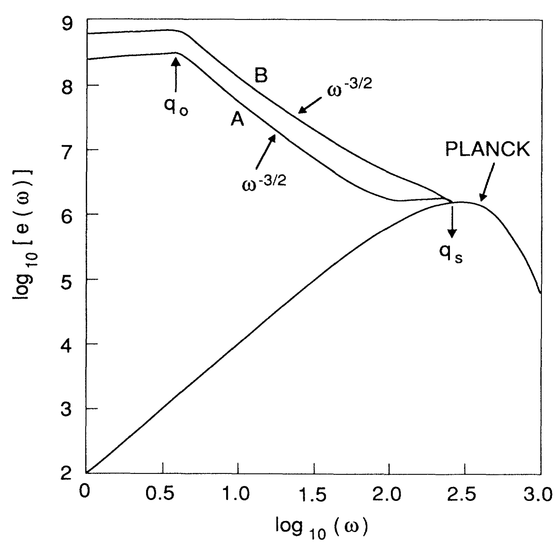

FIG. 4. Forward cascade of energy from the classical regime to nonlinear quantum regime for $q \approx q_c$ and $q > q_c$. In plot A, $q = 6\times10^{19} \approx q_c$; in plot B, $q = 5\times10^{20} > q_c$. In both A and B an energy flux is input over a Gaussian distribution of modes centered at $\omega = 4$ and removed over modes greater than $\omega_p = 280$. Both curves follow a $-\frac{3}{2}$ power law before meeting the initial Planck spectrum with $T = 100$.

and then curves down to meet the Planck spectrum at ω_p.

Above the critical flux the steady-state spectral density is dramatically altered when the sink(s) are situated above ω_p. As shown in Fig. 3, the classical cascade carries past the Planck maximum and then turns down with a slope steeper than Wien's law to meet the Planck spectrum in the quantum domain. We have found that the structure of this distribution is robust in regards to the location of the source and sink, provided that the source is in the classical region and the sink is in the quantum region. The structure of the distribution also remains robust when changing the number of modes from 500 to 2000.

The physics of far off-equilibrium waves (e.g., phonons) differs from the physics of vortex turbulence in that there exits a closed kinetic (Boltzmann type) equation for the time development of the spectral density [6], which furthermore spans both classical and quantum mechanics. In the purely classical domain energy cascades to higher frequency and in the purely quantum domain, there is a reverse cascade of energy to lower frequency. In these cases the steady-state spectra can be evaluated by analytic as well as computational means. In view of the underlying kinetic equation, the "Kolmogorov" constants can be evaluated and the approach to the wave turbulent steady state can be simulated (these aspects of the motion cannot be obtained for vortex turbulence). Simulations have revealed a new (off-equilibrium) nonlinear steady-state spectrum that sits at the interface of classical and quantum mechanics. This state (e.g., Fig. 3) is realized when the input of energy to the low-frequency (i.e., classical) modes is sufficiently high. For instance, we predict that at 1.0 K, energy input at 10 kHz to a high-Q solid (with say $c=10^5$ cm/s and $\rho=5$ g/cm^3) will cascade due to mechanical nonlinearities into the quantum domain if the degree of excitation creates a Mach number M greater than 10^{-3} [note that energy density equals $\rho c^2 M^2 = \int e(\omega) d\omega$; Q stands for "quality factor"]. These quantoclassical turbulent states are described by a new power spectrum for which the analytic theory is yet to be derived. Nevertheless, we predict the possibility of the experimental observation of this new off-equilibrium state.

This research was supported by the U.S. DOE Office of Basic Energy Science Division of Engineering and Geosciences (for S.J.P.) and by the ONR Grant No. N00014-86-0691 (for P. H. R.). The research of M. B. H. was supported by the Hughes Aircraft Company. We are grateful to the Mathematics department at UCLA for generous time allocations on their Alliant *FX*-80 machine. We wish to thank A. Larraza and M. P. Hasselbeck for stimulating discussions.

*Permanent address: Hughes Aircraft Co., Electro-Optical Systems, P.O. Box 902, El Segundo, CA 90245.

[1] D. J. Benney and P. G. Saffman, Proc. R. Soc. London, Ser. A **289**, 301 (1966); A. C. Newell and P. J. Aucoin, J. Fluid Mech. **49**, 593 (1971).

[2] I. M. Khalatnikov, *Introduction to the Theory of Superfluidity* (Benjamin, New York, 1965).

[3] L. D. Landau and I. M. Khalatnikov, *Collected Papers of L. D. Landau,* edited by D. ter Haar (Pergamon, Oxford, 1965), p. 494.

[4] R. Peierls, *Quantum Theory of Solids* (Clarendon, Oxford, 1955).

[5] M. Cabot and S. J. Putterman, Phys. Lett. **83A**, 91 (1981); G. L. Slonimski, Zh. Eksp. Teor. Fiz. **7**, 1457 (1937).

[6] V. E. Zakharov, Zh. Prikl. Mekh. Tekh. Fiz. **4**, 35 (1965) [J. Appl. Mech. Tech. Phys. **6**, 22 (1965)]; V. E. Zakharov, *Basic Plasma Physics,* Vol. 2, edited by M. N. Rosenbluth and R. Z. Sagdeev (Elsevier, New York, 1984), Chap. 5.1, p. 3; R. Kraichnan, Phys. Fluids **11**, 265 (1968); R. Z. Sagdeev, Rev. Mod. Phys. **51**, 1 (1979).

[7] A. N. Kolmogorov, Dokl. Acad. Sci. URSS **30**, 301 (1941).

[8] A. Larraza, S. L. Garrett, and S. Putterman, Phys. Rev. A **41**, 3144 (1990).

[9] A. Larraza, Ph. D. thesis, UCLA, 1987.

[10] U. Happek, Y. Ayant, R. Buisson, and K. F. Renk, Europhys. Lett. **3**, 1001 (1987).

[11] W. E. Bron and W. Grill, Phys. Rev. B **16**, 5303 (1977).

[12] S. J. Putterman and P.H. Roberts, Phys. Rep. **168**, 209 (1988).

[13] L. Kazakovtsev and Y. B. Levinson, Phys. Status Solidi B **96**, 117 (1979); W. L. Schaich, Solid State Commun. **49**, 55 (1984).

[14] S. L. Musher, Phys. Lett. **70A**, 361 (1979).

[15] V. E. Zakharov and S. L. Musher, Dokl. Akad. Nauk SSSR **209**, 1063 (1973).